

# Misorientation behavior of an aluminum bicrystal with 15.7° symmetric tilt boundary using simple shear

Jui-Chao Kuo · Delphic Chen · Shih-Heng Tung ·  
Ming-Hsiang Shih

Received: 18 January 2007 / Accepted: 12 March 2007 / Published online: 3 June 2007  
© Springer Science+Business Media, LLC 2007

**Abstract** The misorientation behavior was investigated in the region of a symmetrical tilt  $\langle 112 \rangle$  boundary with a misorientation of 15.7°. The strain and orientation distributions were obtained by DIC (digital-image-correlation) and EBSD (electron backscattering diffraction) techniques to characterize the kinematical behavior of the grain boundary. In order to obtain a misorientation gradient, the misorientation was used in representation of the axis–angle description. This formation of the orientation gradient is found to have a common rotation axis in the  $[11\bar{2}]$  direction.

## Introduction

The structure of grain boundary plays an important role in influencing deformation mechanisms of bicrystals and polycrystals and this has been of intense interest for many

decades [1]. From the previous studies, it is concluded that the heterogeneity at the meso-scale reveals a nature of inter-granular [2–4] and intra-granular incompatibility [5, 6] due to the presence of grain boundaries. At the microscopic scale grain boundaries can be regarded as a source of dislocations and as an obstacle for the movement of dislocations [1]. These interactions will determine the patterns of lattice curvature observed in the vicinity of grain boundaries and the curvature change may be assumed as the geometrically necessary dislocation (GND) distribution [7].

Although there are a number of experimental investigations on the influence of the grain boundary structure, the grain boundary structure on the mechanical response of a GB is not fully understood at the mesoscale. However, real material behavior has not yet been fully realized. In order to compare with the experimental results, Taylor model provides a simple approach to predict approximately the deformation textures but it fails to meet the predicted intensities of the preferred orientation [8–10]. Taylor [11] assumed that the plastic strain of each grain within a polycrystal is the same and equal to the macroscopic plastic strain of the specimen. In addition, the interaction between the grains is not considered in all Taylor-type models. From this viewpoint Taylor's model is considered as an ideal condition without taking the influence of grain boundary into account. The purpose of this paper is to investigate the local misorientation behavior at the grain boundary during simple shearing by integrating EBSD (electron backscattering diffraction) and DIC (digital-image-correlation) techniques. In contrast to nanocrystalline metals, an aluminum bicrystal with symmetrical  $\langle 112 \rangle$  tilt boundaries at 15.7° was used and the investigated area was close to the grain boundary.

---

J.-C. Kuo (✉) · D. Chen  
Department of Materials Science and Engineering,  
National Cheng Kung University, Tainan 701, Taiwan  
e-mail: jckuo@mail.ncku.edu.tw

S.-H. Tung  
Department of Civil and Environment Engineering,  
National University of Kaohsiung, Kaohsiung 811, Taiwan

M.-H. Shih  
Department of Construction Engineering, National Kaohsiung  
First University of Science and Engineering, Kaohsiung 824,  
Taiwan

## Experimental

A 99.999% pure aluminum bicrystal with symmetrical  $\langle 112 \rangle$  tilt boundaries at  $15.7^\circ$  was prepared by using a modified Bridgman technique with seed crystals of pre-selected orientations from IMM of RWTH Aachen. The initial orientations of the two single crystals in the bicrystal were ( $74.6^\circ, 36.1^\circ, 52.5^\circ$ ) for C1 and ( $91.4^\circ, 34.1^\circ, 50.8^\circ$ ) for C2, where the Euler angles are given after Bunge's definition. The initial orientations were measured using electron backscatter diffraction as shown in Fig. 1b. This misorientation can be described in term of axis/angle as  $[112]/15.7^\circ$ , where the  $[112]$  axis is parallel to the ND direction. The sample dimensions for the simple shear test were prepared in  $17 \times 3 \times 2 \text{ mm}^3$ , as shown in Fig. 1a. The reference coordinates for the shearing are referred to as rolling direction (RD) for the shear direction, transverse direction (TD) for the direction perpendicular to the shear direction, and normal direction (ND) for the direction normal to the sample surface. The grain boundary was chosen to be parallel to the shear direction, as shown in Fig. 1a.

The in-plane shear distribution was determined on the sample normal surface with an area of  $3.1 \times 2.2 \text{ mm}^2$  using DIC technique. The DIC technique based on the recognition of geometrical change in the gray scale distribution is used to analyze the strain mapping. The simple shear was conducted in SEM at a constant shear rate of  $10^{-6} \text{ m s}^{-1}$ . The strain distribution was analyzed after each step displacement of 0.1 mm up to a displacement of 1.3 mm.

Before and after plastic deformation, the local lattice orientations were performed by using EBSD on an area of  $177 \times 194 \mu\text{m}^2$  across the grain boundary. In order to achieve a high lateral resolution, a scan step size of 600 nm was applied to measure the orientation image map (OIM).

## Results and discussion

### Kinematical behavior of bicrystal

The evolution of the accumulated in-plane shear strain,  $\varepsilon_{xy}$ , shows in Fig. 2 for the aluminum bicrystal after a shear

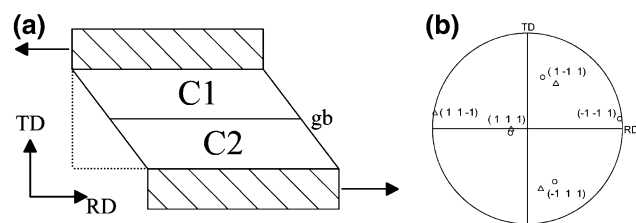


**Fig. 1** (a) Schematic presentation of the experimental setup and the bicrystal. (b)  $\{111\}$  initial pole figure of the bicrystal with a symmetrical tilt grain boundary of  $15.7^\circ$  misorientation, where  $\Delta$  and  $O$  symbol label crystal C1 and crystal C2, respectively

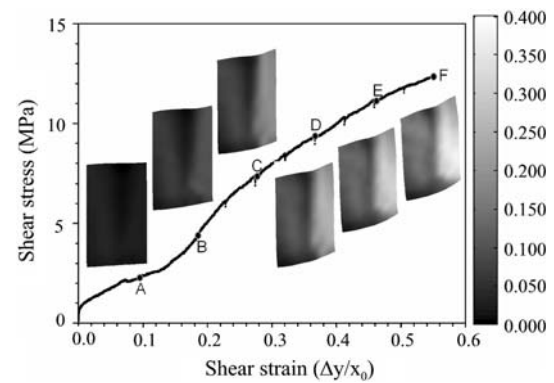


**Fig. 2** The shear strain  $\varepsilon_{xy}$  distribution during simple shear up to a shear strain of 0.56

strain of 0.56. The accumulated shear strain means the shear strain determined from its initial state. It is observed that the two crystals in the bicrystal deform in different magnitude, i.e., asymmetrically. In order to understand the average behavior in each crystal, the average shear strain is calculated by averaging the shear strain of all points for each single crystal, which are determined from DIC. The average shear strain distribution of  $\varepsilon_{xy}$  of the two crystals also reveals this asymmetric deformation in Fig. 3a. The results are in good agreement with those results predicted by the fully constrained Taylor model in Fig. 3b.

During shearing the rotation evolution of the two crystals calculated by the FC Taylor model shows a tendency for the rotation axis to be close to the normal direction and in the counter-clockwise direction as shown in Fig. 4. The phenomenon of the reorientation can be explained as follows. During simple shear deformation, counter shear stress in the lateral direction, i.e., in the transverse direction is needed to obtain the momentum equilibrium. Shear stresses in simple shear deformation exist in the shear direction and in the transverse direction. Therefore, the highest resolved shear stress results on the plane parallel to the shear direction or to the transverse direction [12, 13].

The initial orientations of two single crystals are symmetrical about the  $\langle 112 \rangle$  axis with the misorientation of  $15.7^\circ$ . This reorientation during shearing gives rise to the formation of asymmetrical orientations of the two crystals. In case of the  $(11\bar{1})$  plane the crystal C1 rotates further away from the shear direction than the crystal C2, while in case of the  $(1\bar{1}1)$  plane the crystal C1 rotates closer to the transverse direction as shown in Fig. 4. Therefore, the main activated slip system can be changed from the initial slip system  $(11\bar{1})[1\bar{1}0]$  to the slip system  $(1\bar{1}1)[\bar{1}01]$  for the C2 crystal. In addition to the changing of slip systems, the reorientation can also lead to the formation of different shear strain, because the orientations of bicrystal are not symmetrical. Figure 3a shows that the magnitude of shear

**Fig. 3** (a) The average shear strain  $\epsilon_{xy}$  of both single crystals C1 and C2 in the bicrystal up to a shear strain of 0.56 with the help of DIC technique, (b) the accumulated plastic shear strain obtained by using the FC Taylor model with each step at an increment of 0.025 up to a shear strain of 0.48

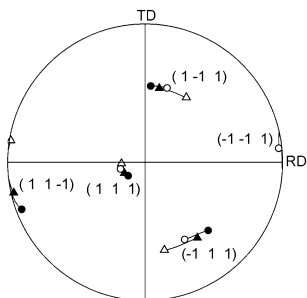
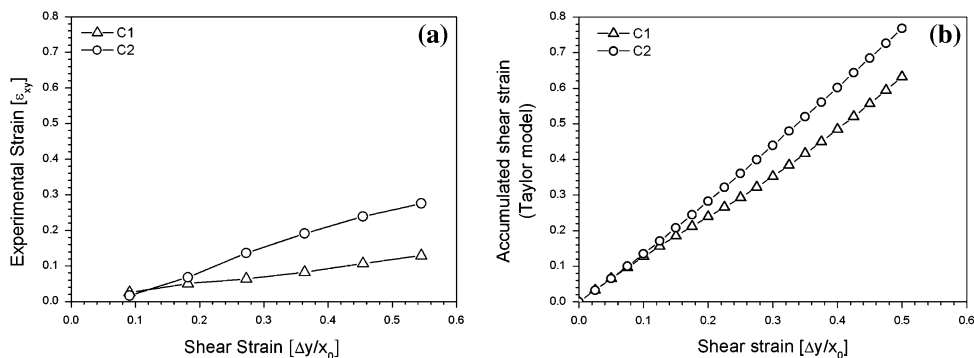


**Fig. 4** {111} Pole figure showing the lattice rotation obtained by using FC Taylor theory. (The  $\Delta$  symbol and  $O$  symbol label the initial orientations of crystal C1 and C2 before shearing, respectively. The solid  $\Delta$  symbol and  $O$  symbol label the final orientations of crystal C1 and C2 after shearing, respectively. Dotted lines represent the orientation evolution)

for C2 crystal is larger than that for C1 crystal after 0.2 shear strain. The slip system  $(1-11)[\bar{1}01]$  parallel to the shear direction contributes to the shear strain much more than the slip system  $(11\bar{1})[1\bar{1}0]$  perpendicular to the shear direction. It is observed in Fig. 5 that for C1 and C2 crystals the Schmid's factor varies its value during simple shearing due to the reorientation. For C1 crystal the maximal value of Schmid's factor is from  $(1-1-1)[110]$  to  $(1-1-1)[01\bar{1}]$  and for C2 crystal it is still  $(1-11)[110]$ . This supports that the change of slip systems and the forming the asymmetrical orientation can be explained the forma-

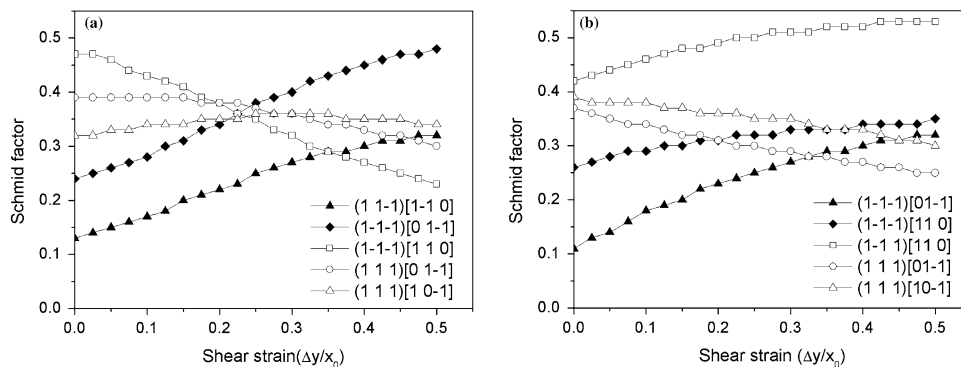
tion of the asymmetric deformation pattern of the bicrystal at the macroscopic observation.

### Misorientation behavior at the grain boundary

The observed feature of microstructures by automatic crystal orientation mapping in Fig. 6a is the formation of parallel block patterns in the upper crystal C1, which lie at an angle of  $53^\circ$  to the shear direction. Two kinds of block patterns indicated as B1 and B2 in the lower crystal C2 lie at the angle of  $53^\circ$  and  $21^\circ$  to the shear direction, respectively. The block patterns of A1, B1 and B2 are not exact parallel to the slip planes  $(1-11)$  and  $(11-1)$ . After the LEDS concept (low energy dislocation structures) [14], the different combinations of polyslip contribute to the splitting of orientation in different blocks. Each block does not correspond to a single crystallographic slip plane because it comprises more than one slip system, i.e. 3–4 slip systems. Thus, the blocks deviate from the crystallographic slip planes.

In addition to the orientation map, the {111} pole figure measured by EBSD in Fig. 4 is in good agreement with that predicted by the fully constrained Taylor model in Fig. 3b. It shows a tendency for the rotation axis to be close to the normal direction and in the counter-clock direction at the grain boundary. It is impossible to extract the behavior of grain boundary from the results of the rotation direction in

**Fig. 5** Schmid's factor of (a) C1 and (b) C2 crystal in the bicrystal by using the FC Taylor model with each step at an increment of 0.025 up to a shear strain of 0.50



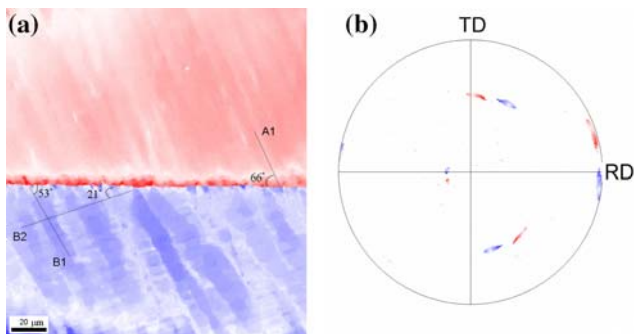


**Fig. 6** (a) The misorientation mapping and (b) the corresponding (111) pole figure close to the grain boundary, where the red and blue colors label the orientations of the upper crystal C1 and of the lower crystal C2, respectively

the pole figures. Therefore, the average misorientation [15] is also used to quantify the misorientation behavior near grain boundary. The misorientation of each measurement point was calculated in comparison to a fixed reference orientation, which refers to the average orientation of the whole area in each crystal of the bicrystal. Subsequently, the average misorientation of all points along straight lines parallel to the grain boundary was determined by calculating the arithmetic mean of the misorientation angle of these points. It is clear that a strong orientation change occurred across the grain boundary after shearing as shown in Fig. 7.

Then, it comes a question if there exists a rotation axis being parallel to any direction of dislocation line on the  $\{111\} \langle 110 \rangle$  slip system. In order to find the rotation axis, the misorientation is described as axis/angle and a reference orientation is necessary. The orientation of each point, at a distance of 80  $\mu\text{m}$  measured from the grain boundary, was chosen as the reference orientation for the C1 crystal. The orientation of each reference point was used to determine the misorientation, in terms of the axis–angle representation, with respect to the orientation of its nearest neighbor, which is parallel to and at a distance varying from 0 to 98  $\mu\text{m}$  from the grain boundary in the crystal C1. From the results of the axis–angle description it is found that most of the rotation axis is parallel to  $[11\bar{2}]$ . Therefore, the number of the misorientation axis being parallel to  $[11\bar{2}]$  is divided by the total number of points at a constant distance from the grain boundary and this is defined as the fraction percentage of the misorientation axis. Figure 8 shows the fraction of the misorientation axis of the  $[11\bar{2}]$  direction calculated for each line with respect to the distance varying from 0 to 98  $\mu\text{m}$  from the grain boundary. This misorientation axis of  $[11\bar{2}]$  is different from the initial misorientation axis of  $[112]$  between the two single crystals. It is clear that the rotation axis is parallel to the  $[11\bar{2}]$  direction, i.e., the direction of the

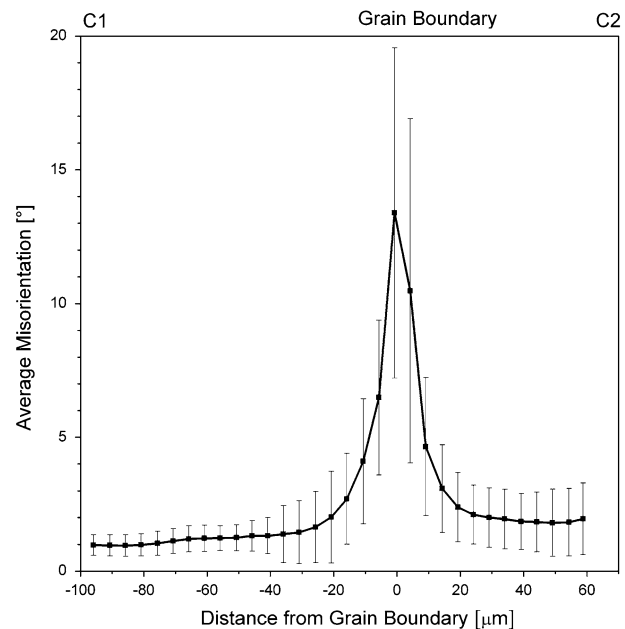


**Fig. 7** Misorientation with respect to the average crystal orientation integrated over narrow stripe-shaped areas parallel to the grain boundary as a function of the distance of the integration area to the grain boundary

dislocation line on the  $(111)[\bar{1}10]$  slip system. In addition, the maximum peak of the fraction of the rotation axis exists at a distance of 5  $\mu\text{m}$  from the grain boundary. This observation suggests that the pile-up of dislocations on the  $(111)[\bar{1}10]$  slip system occurs at the grain boundary. In the case of the C2 crystal, however, the same process was performed for the reference orientation of the points at a distance of 40  $\mu\text{m}$ . It is impossible to observe any misorientation axis at the side of the C2 crystal.

At the initial stage of plastic deformation, mobile dislocations are formed on the slip system with the largest

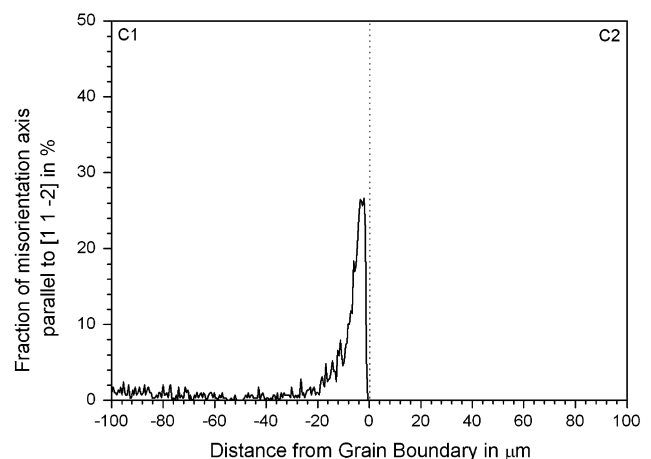


**Fig. 8** Fraction of the misorientation axis parallel to the  $[11\bar{2}]$  direction in crystal C1

local resolved shear stress in the grain [1, 16, 17]. Mobile dislocations, encountering a grain boundary, will pile up before the grain boundary which results in a local stress state and also in an orientation gradient. The larger the misorientation of grain boundary is, the more difficult dislocations cannot penetrate through grain boundaries. Our previous study [18] on an aluminum bicrystal with a symmetric tilt boundary of  $8.7^\circ$  also indicates the occurrence of dislocations pile-ups at the grain boundary. The rotation axis in the direction of  $[1-2-1]$  for the misorientation of  $8.7^\circ$  is different from that of  $[11-2]$  for  $15.7^\circ$ . It is to the contract that dislocations can easily penetrate through a low angle grain boundary. The observations in the proceeding study is due to the reorientation during shearing which results in activating different slip systems in both grains. In this case these two slip systems are perpendicular and thus dislocation pile-ups are built at grain boundaries.

As described in the above, the increasing in the misorientation leads to pile-up for dislocations. Clark et al. [19] showed experimentally that at very low plastic strains dislocation pile-ups can be observed in the vicinity of grain boundaries by transmission electron microscopy. It was observed in the previous study [15] that dislocation pile-ups occur at medium and large angle symmetric tilt boundaries during plane-strain up to 30% reduction in thickness for aluminum bicrystals. Dislocations can penetrate through low angle boundaries with a misorientation  $>15^\circ$ , while it is in contrast for high angle boundaries with a misorientation  $>15^\circ$  [16, 17].

## Conclusions

In this study a pure aluminum bicrystal with symmetrical  $\langle 112 \rangle$  tilt boundaries at  $15.7^\circ$  was sheared up to a shear strain of 0.56. It is observed at the mesoscale an asymmetric deformation pattern from the microstrain mapping and the formation of an asymmetric deformation pattern could result from the reorientation of the two crystals in the

bicrystal during shearing. There exists a misorientation gradient at the microscale in the vicinity of the grain boundary and the length of its influenced zone is about  $20 \mu\text{m}$ . The formation of the misorientation gradient is found to have a common rotation axis in the  $[11-2]$  direction at the side of the crystal C1. This observation suggests that dislocations pile up on the  $(111)[-110]$  slip system.

**Acknowledgements** The authors thank Prof. D. Raabe (MPI Germany) for supplying OIM analysis measurement, Dr. M. Winning (MPI Germany) for providing the bicrystal specimen. J.C. Kuo is grateful for Dr. S. Zaefferer (MPI Germany) for enlightening discussions. This work was funded by the program of National Science Council under project number NSC 94-2216-E-006-031.

## References

1. Sutton A, Balluffi R (1999) *Interface in crystalline materials*. Clarendon Press, Cambridge, UK, p 704
2. Livingston JD, Chalmers B (1957) *Acta Metall* 5:322
3. Hook RE, Hirth JP (1967) *Acta Metall* 15:535
4. Hook RE, Hirth JP (1967) *Acta Metall* 15:1099
5. Rey C, Zaoui A (1980) *Acta Metall* 28:687
6. Rey C, Zaoui A (1982) *Acta Metall* 30:523
7. Sun S, Adams BL, King W (2000) *Phil Mag* A80:9
8. P Van Houtte, Delannay L, Samajdar I (1999) *Textures Microstruct* 31:109
9. P Van Houtte, Li S, Engler O (2004) *Aluminium* 80:702
10. P Van Houtte, Li S, Seefeldt M, Delannay L (2005) *Int J Plasticity* 21:589
11. Taylor GI (1938) *J Inst Metals* 62:307
12. Yamakov V, Wolf D, Phillpot SR, Mukherjee AK, Gleiter H (2004) *Nat Mater* 3:43
13. H Van Swygenhoven, Derlet PM, Froseth AG (2004) *Nat Mater* 3:399
14. Bay B, Hughes N, Hansen D (1992) *Acta Metall Mater* 40:205
15. Zaefferer S, Kuo JC, Zhao Z, Winning M, Raabe D (2003) *Acta Mater* 51:4719
16. Livingston JD, Chalmers B (1957) *Acta Metall* 5:322
17. Lee TC, Robertson IM, Birnbaum HK (1990) *Metall Trans* 21A:2437
18. Chen D, Kuo JC, Tung SH, Shih MH (2007) *Mater Sci Eng A* (in press)
19. Clark WAT, Wagoner RH, Shen ZY, Lee TC, Robertson IM, Birnbaum HK (1992) *Scripta Metall* 26:203